HAL open science

Influence of boundary conditions on the optimization of a geothermal heat pump studied using a thermodynamic model

A Arz, A Minghini, Michel Feidt, M Costea, Christian Moyne

▶ **To cite this version:**

A Arz, A Minghini, Michel Feidt, M Costea, Christian Moyne. Influence of boundary conditions on the optimization of a geothermal heat pump studied using a thermodynamic model. IOP Conference Series: Earth and Environmental Science, 2022, 960 (1), pp.012003. 10.1088/1755-1315/960/1/012003 . hal-03531960

HAL Id: hal-03531960

https://hal.science/hal-03531960v1

Submitted on 18 Jan 2022

HAL is a multi-disciplinary open access archive for the deposit and dissemination of scientific research documents, whether they are published or not. The documents may come from teaching and research institutions in France or abroad, or from public or private research centers.

L'archive ouverte pluridisciplinaire **HAL**, est destinée au dépôt et à la diffusion de documents scientifiques de niveau recherche, publiés ou non, émanant des établissements d'enseignement et de recherche français ou étrangers, des laboratoires publics ou privés.

Distributed under a Creative Commons Attribution 4.0 International License

IOP Conference Series: Earth and Environmental Science

PAPER • **OPEN ACCESS**

Influence of boundary conditions on the optimization of a geothermal heat pump studied using a thermodynamic model

To cite this article: A Arz *et al* 2022 *IOP Conf. Ser.: Earth Environ. Sci.* **960** 012003

View the article online for updates and enhancements.

You may also like

- Geothermal heat in a heat pump use
A Pavlova, J Hansen, H Obermeyer et al.
- Advanced concepts and solutions for geothermal heating applied in Oradea, Romania
C Antal, F Popa, M Mos et al.
- New generation of theoretical models for the thermal response of geothermal heat exchangers
Miguel Hermanns

This content was downloaded from IP address 194.167.7.54 on 10/01/2022 at 14:38

Influence of boundary conditions on the optimization of a geothermal heat pump studied using a thermodynamic model

A Arz[1], A Minghini[1], M Feidt[1], M Costea[2] and C Moyne[1]

[1]L.E.M.T.A., Lorraine University, 2 avenue de la Forêt de Haye, 54516 Vandoeuvre-Lès-Nancy, France
[2]Engineering Thermodynamics Department, University Politehnica of Bucharest, 313 Splaiul Independentei, 060042 Bucharest, Romania

E-mail: monica.costea@upb.ro, https.orcid.org/0000-0002-0954-7286

Abstract. This paper is the logical follow-up to a work [1] whose results were presented at the 28th French Thermal Congress which was to be held in Belfort in 2020. The model developed at that time is completed in this proposal to consider the specificity of the geothermal heat pump. This is a machine operating upon a mechanical vapor compression cycle, the limit of which is an inverse Carnot cycle. Its specificity consists of a cold loop at the source with the geothermal exchanger and the evaporator, then a hot loop at the sink with the condenser and a floor heat exchanger in the application considered here. We are particularly concerned with the optimal sizing of these heat exchangers through their effectiveness. The parametric sensitivity of this distribution to various boundary conditions is studied, especially by focusing on different conditions at the source: (1) imposed soil temperature, corresponding to a Dirichlet condition, (2) imposed heat flux (including adiabatic case), corresponding to a Neumann condition, (3) imposed mechanical power consumed by the heat pump, and (4) imposed coefficient of performance COP, to all cases being associated a finite thermal capacity in thermal contact with the geothermal exchanger operating in steady-state conditions.

1. Introduction

1.1. First models of reverse cycle machines

The first models of reverse cycle machines were developed based on equilibrium thermodynamics and they describe machines with two thermal reservoirs. These reservoirs are in fact thermostats, namely source and sink of infinite thermal capacity and therefore, temperatures T_{CS} = const will be associated to the source and respectively T_{HS}, to the sink [2].

The simultaneous use of energy and entropy balances for a reverse Carnot cycle (refrigerating machine-RM, or heat pump-HP) leads to a limiting value of the First Law efficiency for the machine in

Content from this work may be used under the terms of the Creative Commons Attribution 3.0 licence. Any further distribution of this work must maintain attribution to the author(s) and the title of the work, journal citation and DOI.
Published under licence by IOP Publishing Ltd

the reversible case (according to figure 1: cycle 1-2_{is}-3_{is}-4). The energy balance on a machine cycle is written as:

$$W = Q_{HS} - Q_{CS} \tag{1}$$

where Q_{HS}, thermal energy output from the hot loop,
Q_{CS}, thermal energy input in the cold loop,
W, mechanical energy expense.

The entropy balances on the cycle expressed by using the entropy method is:

$$\frac{Q_{HS}}{T_{HS}} = \frac{Q_{CS}}{T_{CS}} + \Delta S_I \tag{2}$$

with ΔS_I, entropy production due to internal irreversibilities of the cycle.

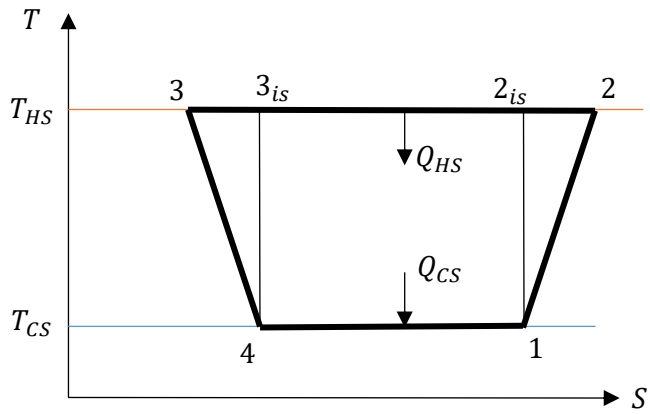

Figure 1. Reverse Carnot cycle: endo-reversible (1-2_{is}-3_{is}-4) or endo-irreversible (1-2-3-4).

As the study focuses on heat pumps, we recall here the coefficient of performance expression for a heat pump

- at imposed mechanical power $\dot{W}_0$:

$$COP_{PAC} = COP_{PAC_{rev}}\left(1 - \frac{T_{CS}\,\dot{S}_I}{\dot{W}_0}\right) \tag{3}$$

- at imposed calorific power $\dot{Q}_{H_0}$:

$$COP_{PAC} = COP_{PAC_{rev}}\left(1 - \frac{T_{CS}\,\dot{S}_I}{\dot{Q}_{H_0}}\right) \tag{4}$$

1.2. The model of the geothermal heat pump

The model of the geothermal heat pump is an advanced version of the previous scheme, comprising a cold loop and a hot loop, as illustrated in figure 2. It is assumed that these two loops operate adiabatically (without thermal losses) so that in steady-state regime one gets:

$$\dot{Q}_g = \dot{Q}_{evap} \;;\; \dot{Q}_{cond} = \dot{Q}_p \tag{5}$$

with $\dot{Q}_g$, thermal power of the geothermal heat exchanger,

$\dot{Q}_{evap}$, thermal power of the evaporator,

$\dot{Q}_{cond}$, thermal power of the condenser and

$\dot{Q}_p$, thermal power of the heating floor at the hot end.

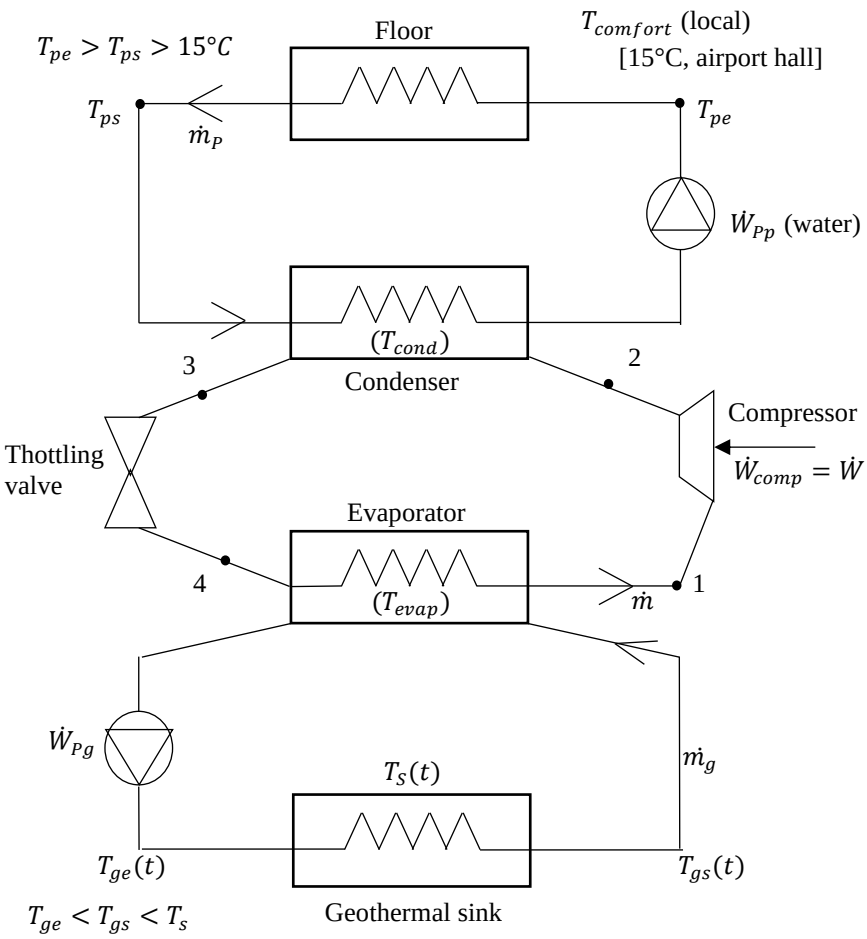

Figure 2. Theoretical scheme of a heat pump model in simple configuration.

The temperatures relative to this configuration and their variation ranges are shown in figure 2, together with the mass flow rates and thermal capacity rates of cold loop fluid $\dot{m}_g$, $\dot{c}_g = \dot{m}_g c_{p_g}$, then of hot loop fluid $\dot{m}_p$, $\dot{c}_p = \dot{m}_p c_{p_p}$. We notice a formal symmetry between the hot end and the cold end loops.

1.3. The influence of finite physical dimensions on the behavior of the heat pump

If we assume the geothermal source of infinite extension [3] the cylindrical geometry of the geothermal sink admits an isothermal type limiting condition:

$$\lim_{R\to\infty} T_s(R) = T_s$$

where T_S is the soil temperature.

If we observe the practical realization (example of Zurich airport), the presence of a set of sources under the building leads rather on a square mesh to a limiting condition of adiabatic type $\left(-\lambda_s \frac{\partial T_s}{\partial x} = 0\right)$. We assume that this condition is well approximated by keeping the cylindrical geometry of the source. The heat pump itself can introduce finiteness conditions if we assume for example the imposed mechanical power $\dot{W}_0$. We can also consider an imposed heat extraction flow $\dot{Q}_0 = \dot{Q}_{evap}$, which leads to impose a constant heat flow from the geothermal source.

One of the objectives of this study is to quantify the influence of boundary conditions on the behavior of the heat pump (sizing and transient behavior over a heating season). Whatever the geothermal exchanger used (single tube, U tubes, bayonet exchanger), four cases will be considered: T_S = ct; $\dot{Q}_0$ imposed; $\dot{W}_0$ imposed, and COP_0 imposed, with the consequences on a possible optimal dimensioning of the heat pump, through a study of parametric sensitivity.

2. Simplification of the study to the Chambadal model

2.1. The geothermal heat pump of Chambadal

Figure 3 illustrates the simplified scheme of the Chambadal geothermal heat pump.

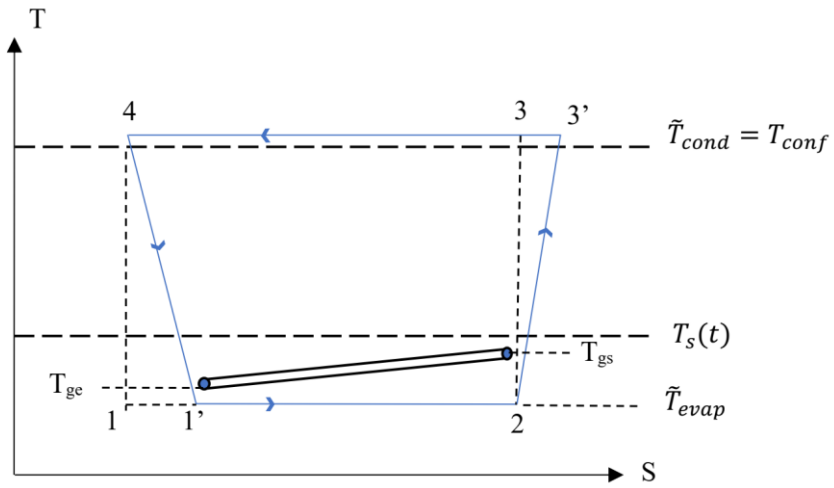

Figure 3. Diagram of the Chambadal geothermal heat pump.

It can be seen in this figure that the high temperature loop is assumed to be perfect, and therefore the set point temperature T_{conf} is identical to the temperature of the condenser.

2.1.1. Cases where T_S is assumed constant [2]

At imposed flow rate and geometry, one gets:

$$\dot{Q}_g = \varepsilon_g \dot{c}_g (T_s - T_{ge}) \tag{6}$$

where T_{ge}, temperature of the geothermal source fluid at the inlet of the heat exchanger,
ε_g, effectiveness of the geothermal source exchanger.

The temperature T_{ge} appears from (6) as a control variable. Then, one can show that the average evaporator temperature is:

$$\tilde{T}_{evap} = T_{ge} - (T_s - T_{ge})\varepsilon_g \left(\frac{1}{\varepsilon_{evap}} - 1\right) \tag{7}$$

The energy balance and the entropic balance of the endo-reversible cycle provide:

$$\dot{Q}_{cond} = \dot{Q}_g + \dot{W} \tag{8}$$

$$\frac{\dot{Q}_g}{\tilde{T}_{evap}} = \frac{\dot{Q}_{cond}}{T_{conf}} \tag{9}$$

Then, the mechanical power expense results in:

$$\dot{W} = \varepsilon_g \dot{c}_g (T_s - T_{ge}) \left[\frac{T_{conf}}{T_{ge} - (T_s - T_{ge})\varepsilon_g \left(\frac{1}{\varepsilon_{evap}} - 1\right)} - 1\right] \tag{10}$$

with ε_{evap}, effectiveness of the evaporator.

The expression of $\dot{W}$ appears as an increasing function of ($T_S - T_{ge}$), decreasing of T_{ge}, increasing of ε_g, ε_{evap}, and with the finite physical dimension constraint of ε_g, + $\varepsilon_{evap} = \varepsilon_g \leq 2$, an optimal distribution should result.

2.1.2. Cases where $\dot{Q}_g$ is assumed constant $(\dot{Q}_0)$

Unlike the isothermal condition (or Dirichlet condition) imposed in the previous subsection, this second condition corresponds to an extensive or Neumann condition. Hence it comes:

$$T_{ge} = T_s - \frac{\dot{Q}_o}{\varepsilon_g \dot{c}_g} \tag{11}$$

$$\tilde{T}_{evap} = T_s - \frac{\dot{Q}_o}{\dot{c}_g}\left(\frac{1}{\varepsilon_g} + \frac{1}{\varepsilon_{evap}} - 1\right) \tag{12}$$

The combination of the energy and entropy balances with the two preceding expressions leads to:

$$\dot{W} = \dot{Q}_o \left[\frac{T_{conf}}{T_s - \frac{\dot{Q}_o}{\dot{c}_g}\left(\frac{1}{\varepsilon_g} + \frac{1}{\varepsilon_{evap}} - 1\right)} - 1\right] \tag{13}$$

This function is increasing by $\dot{Q}_o$ and decreasing by T_S. But for T_S and $\dot{Q}_o$ parameters, it appears that the effectiveness finiteness constraint leads, under endo-reversible conditions, to the distribution of ε_g, ε_{evap} related by:

$$\dot{\varepsilon}_g^* = \dot{\varepsilon}_{evap}^* = \frac{\varepsilon_T}{2} \tag{14}$$

The minimum mechanical power expense under endo-reversible conditions becomes:

$$min\ (\dot{W}) = \dot{Q}_o \left[\frac{T_{conf}}{T_s - \frac{\dot{Q}_o}{\dot{c}_g}\left(\frac{4}{\varepsilon_T} - 1\right)} - 1\right] \tag{15}$$

2.1.3. Cases where $\dot{W}$ is assumed constant $(\dot{W}_0)$

The combination of the energy and entropy balances with the imposed mechanical power $\dot{W}_0$ constraint provides:

$$\dot{Q}_g = \dot{W}_0 \frac{\tilde{T}_{evap}}{T_{conf} - \tilde{T}_{evap}} \tag{16}$$

where the average temperature over the evaporator has the expression given in section 2.1.2:

$$\tilde{T}_{evap} = T_{ge} - \frac{\dot{Q}_g}{\dot{c}_g}\left(\frac{1}{\varepsilon_{evap}} - 1\right) \tag{17}$$

Equation (17) depending on $\dot{Q}_g$ has to be solved if T_{ge} is a control variable. Otherwise, if T_S is imposed by the source, the corresponding equation to solve will be:

$$\tilde{T}_{evap} = T_s - \frac{\dot{Q}_g}{\dot{c}_g}\left(\frac{1}{\varepsilon_g} + \frac{1}{\varepsilon_{evap}} - 1\right) \tag{18}$$

Then, equation (16) becomes a new second order equation expressed by:

$$\dot{Q}_g = \frac{(T_{conf} - T_S) + \frac{\dot{W}_0}{\dot{c}_g}\left(\frac{1}{\epsilon_g} + \frac{1}{\epsilon_{evap}} - 1\right) + \sqrt{\Delta}}{\frac{2}{\dot{c}_g}\left(\frac{1}{\epsilon_g} + \frac{1}{\epsilon_{evap}} - 1\right)} \tag{19}$$

with

$$\Delta = \left[\left(T_{conf} - T_S\right) + \frac{\dot{W}_0}{\dot{c_g}}\left(\frac{1}{\epsilon_g} + \frac{1}{\epsilon_{evap}} - 1\right)\right]^2 + \frac{4\dot{W}_0}{\dot{c_g}} T_S \left(\frac{1}{\epsilon_g} + \frac{1}{\epsilon_{evap}} - 1\right)$$

A possible approximation is provided by the following expression:

$$\dot{Q}_g \approx \dot{W}_0 \frac{T_S}{\left(T_{conf} - T_S\right) + \frac{\dot{W}_0}{\dot{c_g}}\left(\frac{1}{\epsilon_g} + \frac{1}{\epsilon_{evap}} - 1\right)} \tag{20}$$

Note that under the endo-reversibility and approximation conditions, the maximum of $\dot{Q}_g$ is obtained at the effectiveness equipartition:

$$Max\left(\dot{Q}_g\right) \approx \dot{W}_0 \frac{T_S}{\left(T_{conf} - T_S\right) + \frac{\dot{W}_0}{\dot{c_g}}\left(\frac{4}{\epsilon_T} - 1\right)} \tag{21}$$

2.1.4. Case where COP is imposed (COP_0)

One easily finds that COP_0 of the heat pump that is given by:

$$COP_0 = \frac{T_{conf}}{T_{conf} - T_{evap}} \tag{22}$$

with

$$T_{evap} = T_S - \frac{\dot{Q}_g}{\dot{c_g}}\left(\frac{1}{\epsilon_g} + \frac{1}{\epsilon_{evap}} - 1\right) \tag{23}$$

By combining equations (22) and (23) and setting $z_0 = \frac{COP_0 - 1}{COP_0}$, the resulting expression of the objectif function $\dot{Q}_g$ is:

$$\dot{Q}_g = \dot{c}_g \frac{T_S - z_0 T_{conf}}{\frac{1}{\epsilon_g} + \frac{1}{\epsilon_{evap}} - 1} \tag{24}$$

Like the result of the previous case, under endo-reversibility conditions, the maximum useful effect corresponds to the maximum of $\dot{Q}_g$ at the equipartition of the effectiveness:

$$Max\left(\dot{Q}_g\right) = \frac{\dot{c}_g}{\frac{4}{\epsilon_T} - 1}\left(T_S - z_0 T_{conf}\right) \tag{25}$$

Equation (25) also implies an inequality condition on T_S expressed by $T_S \geq z_0\, T_{conf}$.

3. Discussions of the Chambadal geothermal heat pump model results

A parametric sensitivity study and the comparison of the 4 previous operating case results when the effectiveness finiteness condition of the geothermal source is considered, will be presented in this section.

3.1. Characteristic of the geothermal heat pump

In addition to the existence of two loops (hot and cold), the geothermal heat pump has a transient source on a seasonal scale (heating or cooling) and moreover, it is finite so that:

$$\dot{Q}_g(t) = -M_s Cp_s \frac{d\bar{T}_s(t)}{dt} = \varepsilon_g \dot{c}_g\left(\bar{T}_s - T_{ge}\right) \tag{26}$$

with $c_s = M_s C_{ps}$, thermal capacity of the finite source in [J/K],

$\bar{T}_s$, average value of the soil temperature.

If the temperature T_{ge} is a parameter (constant control variable), by integrating equation (26) one gets:

$$\frac{\overline{T}_s - T_{ge}}{\overline{T}_s(0) - T_{ge}} = e^{\frac{-t}{\tau_s}}$$

where $\tau_s = \frac{c_s}{\varepsilon_g \dot{c}_g}$ (or $\frac{c_s}{k_g A_g}$), thermal soil time constant.

The thermal soil time constant must be longer than the contact time at each exchanger (on the order of a minute) or the heat pump, so that the heat pump is always considered in steady state operation, while the source is imposing slow transient conditions:

$$\dot{Q}_g(t) = \varepsilon_g \dot{c}_g \left(\overline{T}_s - T_{ge}\right) e^{\frac{-t}{\tau_s}} \tag{27}$$

It is therefore possible, using equation (27), to simulate the operation of the heat pump over a heating season for the various conditions discussed in section 2, and to analyze the sensitivity of this operation with respect to the parameters, in order to get an optimal sizing and a better control of the heat pump operation over time (operation with T_S or T_{ge}, $\dot{c}_g, T_{conf}, \varepsilon_T$ as parameters, $\varepsilon_{évap}, \varepsilon_g$ as variables, and boundary conditions with $\dot{Q}_0, \dot{W}_0, or\ COP_0$ imposed).

3.2. Some results of the Chambadal model of the geothermal heat pump

An illustration of some results corresponding to the analytical expressions derived in section 2 for the cases of the Chambadal model relative to the geothermal heat pump are presented in figures 4-6 (the ordinate axe is given in arbitrary units).

For the case where the COP is imposed (section 2.1.4), figure 4 shows the evolution of the maximum of the $\dot{Q}_{g,arb}$ (dimensionless thermal power input from the geothermal source), as a function of the effectiveness of the geothermal source exchanger, for different values of the overall effectiveness ε_T. A strong influence of ε_T on $\dot{Q}_{g,arb}$ variation is found, as well as effectiveness equipartition ($\varepsilon_g = \varepsilon_{evap} = 0.5$) for $\varepsilon_T = 1$, corresponding to $Max\left(\dot{Q}_{g,arb}\right)$.

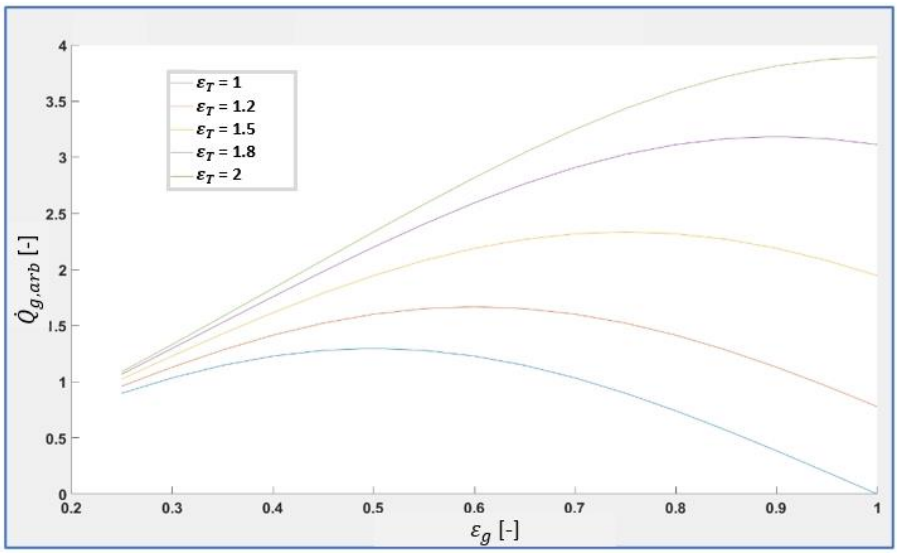

Figure 4. Variation of $\dot{Q}_{g,arb}$ as a function of ε_g for the case with imposed COP_0.

In the case of an imposed $\dot{Q}_g$ at the cold source (section 2.1.2), figure 5 shows the existence of a minimum of the consumed mechanical power $\dot{W}$ as a function of ε_T. Despite of the fact that it is a very flat one, it proves that the sizing optimization through ε_g can be achieved. Also, the curves in figure 5 show that it decreases and moves to higher values of the effectiveness ε_g when the total effectiveness ε_T increases.

The influence of ε_T on the min($\dot{W}$) is small and it is confirmed through figure 6 where min($\dot{W}$) increases significantly with $\dot{Q}_0$, while the total effectiveness ε_T makes the curves distinct only for high value of $\dot{Q}_0$.

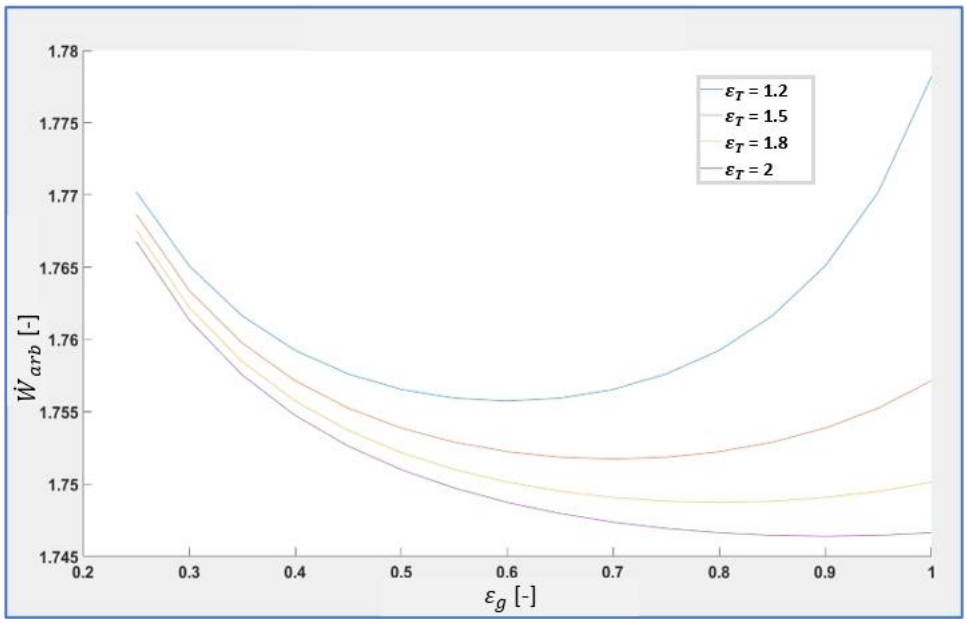

Figure 5. Variation of $\dot{W}_{arb}$ as a function of ε_g for the case with imposed $\dot{Q}_0$.

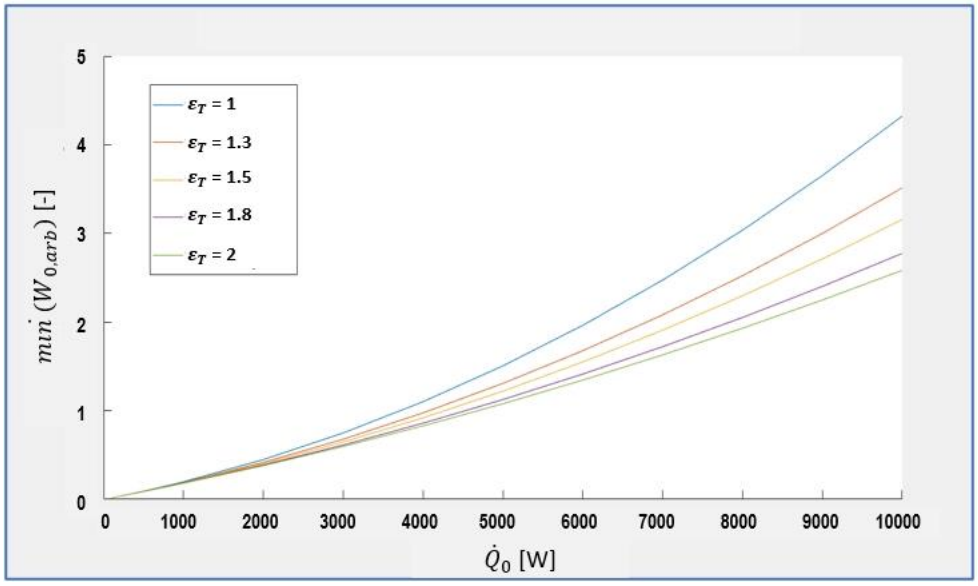

Figure 6. Variation of $min\ \dot{W}_{arb}$ as a function of $\dot{Q}_0$.

In the case of $\dot{W}_0$ imposed and for low values compared with the other heat flows, the following non-dimensional expression is obtained for the thermal power of the geothermal source:

$$\dot{q}_g \approx \frac{\dot{w}_0\, t_s}{1-t_s}\left[1-\frac{\dot{w}_0}{1-t_s}\left(\frac{4}{\varepsilon_T}-1\right)\right] \tag{28}$$

with $\dot{w}_0 = \frac{\dot{W}_0}{\dot{c}_g T_{conf}}$; $t_s = \frac{T_S}{T_{conf}}$.

The equation (28) becomes zero when $\dot{w}_0 = 0$ or $\dot{w}_0 = \frac{1-t_s}{\frac{4}{\varepsilon_T}-1} = \dot{w}_{lim}$.

It results that the maximum of $\dot{q}_g$ will be obtained for $\dot{w}_0 = \frac{\dot{w}_{lim}}{2}$, and will be given by:

$$Max(\dot{q}_g) = \frac{t_s}{2}\left(\frac{1}{\frac{4}{\varepsilon_T}-1}\right) \tag{29}$$

The maximum value of $\dot{Q}_g$ from equation (29) is an increasing function of (T_S, ε_T) from the point of view of operation, and then of ($\dot{c}_g$, T_{conf}) from the point of view of heat exchangers dimensioning.

4. Conclusions and Perspectives

The paper explores the influence of the boundary conditions on the optimum operation and heat exchangers sizing of a geothermal heat pump. The reported elements complete those previously obtained in [1,4].

The modeling of the geothermal heat pump uses a Chambadal-type model well suited for the study and sensitivity analysis of the geothermal source boundaries conditions.

Original results are proposed and discussed. Thus, the existence of a minimum of mechanical power consumed is emphasized for imposed *COP* of the heat pump, respectively a maximum useful effect $\dot{Q}_g$ that is obtained for equipartition of the heat exchangers effectiveness.

In perspective, the extension of this approach to the Curzon-Ahlborn configuration of the heat pump is considered, as well as its validation by comparison with the existing results in the literature.

The extension of the model to the Curzon-Ahlborn configuration of the heat pump is currently developed, and then, its validation by comparison with existing results in the literature will be considered.

References

[1] Gervaise C 2020 Entropic model of a heat pump *Master Thesis Lorraine University* (In French)
[2] Feidt M 2013 *Finite Physical Dimensions Optimal Thermodynamics* (Paris: Hermes-Lavoisier) (In French)
[3] Moyne C and Feidt M 2019 Low-temperature geothermal energy and heat pump *Revue générale du froid et du conditionnement de l'air*, March-April, 38-45 (In French)
[4] Pahud D and Hubbuch M 2007 Measurements and optimization of the installation with energy piles at the Dock Midfield at Zurich Airport *Final Report* (In French)